Estimates of global biomass burning emissions for reactive greenhouse gases (CO, NMHCs, and NO_x) and CO_2

Atul K. Jain,[1] Zhining Tao,[1] Xiaojuan Yang,[1] and Conor Gillespie[1]

Received 18 May 2005; revised 26 October 2005; accepted 2 December 2005; published 22 March 2006.

[1] Open fire biomass burning and domestic biofuel burning (e.g., cooking, heating, and charcoal making) algorithms have been incorporated into a terrestrial ecosystem model to estimate CO_2 and key reactive GHGs (CO, NO_x, and NMHCs) emissions for the year 2000. The emissions are calculated over the globe at a $0.5° \times 0.5°$ spatial resolution using tree density imagery, and two separate sets of data each for global area burned and land clearing for croplands, along with biofuel consumption rate data. The estimated global and annual total dry matter (DM) burned due to open fire biomass burning ranges between 5221 and 7346 Tg DM/yr, whereas the resultant emissions ranges are 6564–9093 Tg CO_2/yr, 438–568 Tg CO/yr, 11–16 Tg NO_x/yr (as NO), and 29–40 Tg NMHCs/yr. The results indicate that land use changes for cropland is one of the major sources of biomass burning, which amounts to 25–27% (CO_2), 25 –28% (CO), 20–23% (NO), and 28–30% (NMHCs) of the total open fire biomass burning emissions of these gases. Estimated DM burned associated with domestic biofuel burning is 3,114 Tg DM/yr, and resultant emissions are 4825 Tg CO_2/yr, 243 Tg CO/yr, 3 Tg NO_x/yr, and 23 Tg NMHCs/yr. Total emissions from biomass burning are highest in tropical regions (Asia, America, and Africa), where we identify important contributions from primary forest cutting for croplands and domestic biofuel burning.

Citation: Jain, A. K., Z. Tao, X. Yang, and C. Gillespie (2006), Estimates of global biomass burning emissions for reactive greenhouse gases (CO, NMHCs, and NO_x) and CO_2, *J. Geophys. Res.*, *111*, D06304, doi:10.1029/2005JD006237.

1. Introduction

[2] Assessing the impact of human activities on climate change requires not only accurate emission estimates of major greenhouse gases (GHGs) (e.g., carbon dioxide (CO_2), methane (CH_4), and ozone (O_3)) but also emission estimates of reactive GHGs (e.g., carbon monoxide (CO), nitric oxides (NO_x), and nonmethane hydrocarbon compounds (NMHCs)). Reactive GHGs, although largely transparent to IR radiation, can impact the climate system by altering the concentrations of CH_4 and tropospheric O_3 (two major GHGs) through complex chemical processes [*Prather et al.*, 2001]. A number of studies have emphasized the interactive nature of CH_4 and reactive GHGs, and the effects these interactions can have on overall climate change [*Fuglestvedt et al.*, 1996; *Daniel and Solomon*, 1998; *Kheshgi and Jain*, 1999; *Kheshgi et al.*, 1999; *Hayhoe et al.*, 2000].

[3] Although energy related reactive GHG emissions are relatively well represented in the current emission inventory, uncertainties in emissions from nonenergy sources (e.g., biomass burning, vegetation, soil, ocean, and nonvehicle mobile sources) at the global level are considerably large [*Prather et al.*, 2001]. In particular, biomass burning has been identified as an important source of reactive GHGs since the early 1980s [*Andreae and Merlet*, 2001]. It also plays a central role in carbon cycling through the direct release of CO_2, the single most important anthropogenic GHG, into the atmosphere during biomass burning. At the same time, studies also suggest that fire and logging increases the vulnerability of forests to future burning [*Cochrane et al.*, 1999; *Keeley et al.*, 1999; *Nepstad et al.*, 1999]. Because of the impact that reactive GHG emissions from biomass burning exert on atmospheric chemistry and the carbon cycle, the development of a complete emission inventory is vital to the successful study of global atmospheric chemistry and climate change.

[4] Earlier global modeling estimates of biomass burning emission inventories relied on scattered and incomplete data of available fuel for burning and the percentage of fuel that is actually burned over a specific time period [*Crutzen and Andreae*, 1990; *Hao et al.*, 1990; *Hao and Liu*, 1994; *Lobert et al.*, 1999; *Galanter et al.*, 2000]. The uncertainties of these inventories are considerably high. More recently, the modeling studies have taken advantage of available satellite remote sensing data and/or more comprehensive biogeochemical models to estimate the amount of biomass burned owing to open fire and associated emissions [*van der Werf et al.*, 2003, 2004; *Ito and Penner*, 2004; *Hoelzemann et al.*, 2004].

[5] The purpose of this study is to build upon and extend the approaches of previous studies. While we use the same or similar information for combustion completeness and

[1]Department of Atmospheric Science, University of Illinois, Urbana, Illinois, USA.

0148-0227/06/2005JD006237$09.00

emission factors, we implement these data in our newly developed independent ISAM (Integrated Science Assessment Model) terrestrial ecosystem model to estimate the emissions of reactive GHGs from open fire biomass burning and domestic biofuel burning (e.g., cooking, heating, and charcoal making). The advantage of implementing the biomass emission relationship into the ISAM terrestrial ecosystem model is that we can account for the aboveground and surface fuel removed by land use changes. Although such effects have generally been implicitly calculated in recent modeling studies of biomass burning [*van der Werf et al.*, 2003, 2004; *Ito and Penner*, 2004; *Hoelzemann et al.*, 2004], the land use component has not been systematically determined. This approach includes the influence on fuel load of various ecosystem processes (such as stomatal conductance, evapotranspiration, plant photosynthesis and respiration, litter production, and soil organic carbon decomposition) and important feedback mechanisms (such as the climate and fertilization feedback mechanisms). In this paper, the ISAM terrestrial ecosystem model, along with available data sets for the global area burnt, land use changes, and forest density, have been used to study the global emissions for reactive greenhouse gases (CO, VOCs, and NO_x) and CO_2 emissions in the year 2000. The results are compared with other recently published model results and data-based studies that use similar data sets and modeling approaches. Finally, the sources of uncertainties in various input parameters and model results, and the potential for reduction of these uncertainties are discussed.

2. Methodology

[6] The emission calculations associated with open fires and land clearing for croplands were carried out using the standard method for estimating emissions from biomass burning [*Seiler and Crutzen*, 1980; *Hao et al.*, 1990; *Pereira et al.*, 1999; *Potter et al.*, 2002]. According to this method the total yearly emissions (E_{ij}, Tg/yr) of a gas for vegetation type i within a grid cell j are

$$E_{ij} = [DM]_{ij} \times [CC]_{ij} \times [EF]_{ij},$$

$$DM_{ij} = \sum_{t=1}^{12} \left([A]_{ijt} \times [AFL]_{ijt} \right) \text{ for nonclearing for cropland fires,}$$

$$DM_{ij} = [A]_{ij} \times [B]_{ij} \times [\alpha]_{ij} \quad \text{for clearing for cropland fires,}$$

where DM is the dry matter burned (kg) for vegetation type i within each grid cell j, CC is the combustion completeness or efficiency for vegetation type i within each grid cell j, and EF (g species/kg dry matter) is an emission factor of a gas for an open fire in ecosystem type i of grid cell j, t is the total number of months (t = 12), A (km^2) is the total burnt area or cleared area (km^2) for croplands for each vegetation type i within each grid cell j, AFL (kg dry matter/km^2) is the monthly available fuel load or burnable plant material for vegetation type i within each grid cell j, B (kg/km^2) is the biomass cleared for croplands for vegetation type i within each grid cell j. α is the fractions of total cleared vegetation

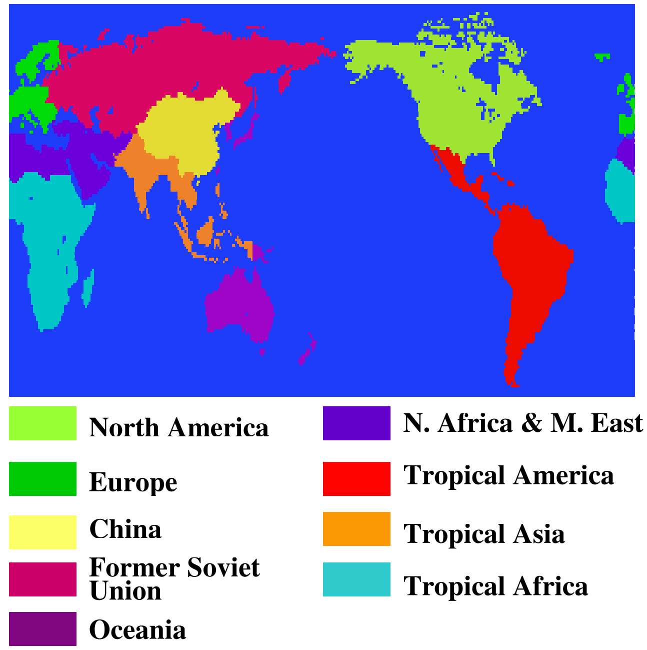

Figure 1. Geographical distributions of the nine regions considered in this study for the regional biomass burning emission analysis.

burned for vegetation type i within each grid cell j. CC and EF considered in this study are also functions of vegetation type and region. The global and annual emissions for CO, NMHCs, and NO_x (as NO) are calculated at 0.5° × 0.5° spatial resolution. B and AFL are calculated using the terrestrial component of the ISAM coupled with the latest forest canopy cover density map produced from the AVHRR 1 km resolution satellite data set [*Zhu and Waller*, 2003]. In order to obtain regional information about the biomass burning related emissions we divided the global land into nine regions, depicted in Figure 1.

2.1. Available Fuel Load

[7] In this study, the global biomass density to determine available fuel load (AFL) or pre-burnable plant material is calculated using the terrestrial component of our ISAM [*Jain and Yang*, 2005]. The model simulates the carbon fluxes to and from different compartments of the terrestrial biosphere with 0.5° × 0.5° spatial resolution. Each grid cell is occupied by at least one of the twelve natural land coverage classifications and/or croplands (for example, a grid cell can contain 50% forest, 30% cropland and 20% grassland) according to the vegetation maps of *Loveland and Belward* [1997] and *Haxeltine and Prentice* [1996], and by at least one of the 105 soil types based on the FAO-UNESCO Soil Map of the World [*Zobler*, 1986, 1999] representing both highly managed and less managed land cover types. We have considered only 10 natural vegetation types and croplands (Table 1). The two other vegetation types, tundra and polar desert, were omitted owing to their insignificance in estimating biomass burning activities. Within each grid cell, the carbon dynamics of each land-coverage classification are described by an ecosystem model consisting of ground vegetation (GV) representing herbaceous carbon reservoirs; nonwoody tree part (NWT)

Table 1. Percentage of Accessible Carbon Vegetation Density (ACVD) Susceptible for Burning for Each Ecosystem Type and Carbon Pool

Land Cover Type	GV	NWT	WT	DPM/RPM[a]
Tropical evergreen	50[b]	50[b]	20[c]	100/30
Tropical deciduous[d]	60	60	24	100/30
Temperate evergreen	50[e]	10[c]	10[c]	100/30
Temperate deciduous[d]	60	12	12	100/30
Boreal	50[e]	25[c]	25[c]	100/30
Savanna	98[f]	0[g]	0[g]	100/0
Grassland	98[f]	0[g]	0[g]	100/0
Pastureland	58[f]	0[g]	0[g]	100/0
Shrubland	98[f]	0[g]	0[g]	100/0
Cropland	98[f]	0[g]	0[g]	100/0

[a]Assume 100% of the accessible biomass of the DPM litter pool is available for burning, while only 30% and 0% of the accessible biomass of RPM is available for burning in forest and nonforests regions, respectively.
[b]*Goldammer and Mutch* [2001].
[c]*Hoelzemann et al.* [2004].
[d]Assume 20% higher than evergreen forests.
[e]*Soja et al.* [2004].
[f]*Shea et al.* [1996].
[g]*Shea et al.* [1996]; *Hoffa et al.* [1999]; *Scholes et al.* [1996].

representing foliage, flowers and roots in transition; woody tree parts (WT) representing branches, boles, and most root material of trees; two litter reservoirs (DPM and RPM, described below), representing litter input from above and below ground litter biomass plant parts; and three soil reservoirs (microbial biomass (BIO), humified organic matter (HUM), and inert organic matter (IOM)). The ISAM terrestrial model also consists of forest clearing and agriculture waste reservoirs. The carbon stored in these reservoirs is released to the atmosphere at a variety of rates depending on usage and is assigned products into three general reservoirs with turnover time of 1 year (agriculture and agriculture products), 10 years (paper and paper products), and 100 years (lumber and long-lived products).

[8] There are many features of this model that make it suitable for estimating fuel loads. First, the separation between ground vegetation (GV) and two tree parts (NWT and WT) allow us to account for the distinct woody and nonwoody biomass variation within each ecosystem type.

[9] Second, distinction between two kinetically defined pools of plant litter, metabolic or decomposable (DPM) and structural or resistant plant material (RPM), allows us to properly account for partially decomposed organic material fuel in the upper portion of the ground surface vegetation. Note that the DPM constitutes the cytoplastic compounds of plant cells and is more susceptible to fires, whereas the RPM represents the cell wall with bound protein and lignified structures and is less susceptible to fires than DPM plant material.

[10] Third, the forest clearing and agriculture waste reservoirs allow us to account for biomass burned through land transformation. Studies suggest that models may be underestimating the total biomass burning emissions owing to omission of these effects [*Scholes et al.*, 1996].

[11] Finally, the ISAM modeling approach allows us to estimate the time dependent *AFL*. Owing to the long turnover times of some of the model reservoirs, the carbon is accumulated over many years to generate the biomass in different terrestrial ecosystem reservoirs. Therefore we first initialized the vegetation model with a 1765 atmospheric CO_2 concentration of 278 ppmv to calculate the equilibrium net primary production (NPP) in addition to vegetation and soil carbon for different model pools. Next, we ran the model at a monthly time step up to the year 2000 using observed monthly temperature and precipitation changes (T. D. Mitchell et al., A comprehensive set of high-resolution grids of monthly climate for Europe and the globe: The observed record (1901–2000) and 16 scenarios (2001–2100), submitted to *Journal of Climate*, 2005) and CO_2 concentrations [*Neftel et al.*, 1985; *Friedli et al.*, 1986; *Keeling and Whorf*, 2000]. We also utilized surveys of past land cover changes due to three types of land cover change activities: clearing of natural ecosystems for croplands and/or pasturelands, recovery of abandoned croplands/pasturelands to preconversion natural vegetation, and production and harvest in conversion areas [*Jain and Yang*, 2005].

[12] In order to account for fire in the ISAM, two modifications were implemented. First, we assume that only surface and aboveground biomass is accessible for burning (i.e., excluding live and dead root material). Part of the above ground dead biomass, such as fine leaf and grass, is entered into the DPM pool and assumed to decay metabolically. The rest of the above ground dead biomass, such as branches and heavy lignified material, enters the RPM pool and is assumed to structurally decompose. The DPM and RPM also contain the belowground dead fine and heavy roots, which are assumed not to be part of the biomass density susceptible to burning. The different resolutions of the two burned data sets (1 km $\times$ 1 km) and the ISAM terrestrial model ($0.5^\circ \times 0.5^\circ$) needed to be integrated, in order to account for spatial variability in forest and non forest biomass at $0.5^\circ \times 0.5^\circ$ resolution. To do this we estimate the fraction of forest and nonforest plant material area within each burned 1-km grid cell using the latest forest canopy cover density map produced from the global forest cover map of the USGS (U.S. Geological Survey) [*Loveland et al.*, 1999], in combination with the AVHHR 1-km data for geographical distribution and conditions of global forest resources [*Zhu and Waller*, 2003]. Next, we sum all forest and nonforest burned plant material area within each $0.5^\circ \times 0.5^\circ$ grid cell. Then we multiply these areas (in m^2) by the corresponding half-degree model-determined burned tree and nontree biomass density (in gC/m^2). The nontree burned density is assigned to herbaceous plants represented by the GV pool, whereas the tree burned biomass density is assigned to the WT and NWT pools.

[13] Using *Zhu and Waller*'s [2003] fractional tree cover map, the global and annual tree-covered burned area detected by the GLOBSCAR and GBA (discussed in section 2.4) products were 442,435 km^2 and 747,000 km^2, respectively. At the same time, GLOBSCAR and GBA products reported global total forest area burned of 307,000 km^2 [*Simon et al.*, 2004], and 700,000 km^2 [*Tansey et al.*, 2004], respectively. Our estimated values for the GLOBSCAR and GBA data are slightly higher than *Simon et al.* [2004] and *Tansey et al.* [2004], respectively, as discussed in section 3.2.

[14] The total preburnt accessible vegetation carbon density for each grid cell is the sum of vegetation density of GV, WT (branches and boles), NWT, DPM, and RPM.

Table 2. Combustion Completeness (*CC*) for Different Land Cover Types

Land Cover Type	Combustion Completeness, %	Source
Tropical evergreen	0.50	*Fearnside* [2000]
Tropical deciduous	0.50	*Fearnside* [2000]
Temperate evergreen	0.50	*Hoelzemann et al.* [2004]
Temperate deciduous	0.50	*Hoelzemann et al.* [2004]
Boreal	0.50	*Hoelzemann et al.* [2004]
Savanna	0.75	Average of *Ward et al.* [1996], *Hoffa et al.* [1999], and *Hély et al.* [2003]
Grassland/Pastureland	0.83	Average of *Hoffa et al.* [1999] and *Fearnside* [2000]
Shrubland	0.75	Average of *Ward et al.* [1996], *Hoffa et al.* [1999], and *Hély et al.* [2003]
Cropland	0.86	*Saarnak et al.* [2003]

Subsequently, the total biomass fuel density from total carbon density is converted by assuming 45% carbon per unit of total biomass for all natural vegetation types and croplands [*Scholes and Walker*, 1993].

[15] Not all of the ISAM estimated accessible vegetation carbon density (g/m^2) (AVCD) is subject to biomass burning. The amount (in%) of AVCD per ecosystem and carbon pool that is available for burning depends mainly on the severity of the fire [*Hély et al.*, 2003; *Lambin et al.*, 2003; *Soja et al.*, 2004]. On a forest stand scale, severity is related to the fire type (i.e., surface or crown), fire intensity, specific forest ecosystem, and weather conditions. Since the two burned data products used in this study only provide the information of the burned area occurrence in terms of "0" (no biomass burning) or "1" (biomass burning) in each 1-km area, rather than the type of fire for area burnt, we are forced to estimate the percentage of AVCD susceptible for burning according to the literature where available and according to our best judgment where necessary. Owing to this limitation with the area burned data, we also do not account for the fire-induced mortality of living biomass. Table 1 provides the percentage of AVCD susceptible for burning for each ecosystem type and carbon pool. Finally, AFL is calculated by multiplying the model estimated AVCD by the percentage values given in Table 1.

2.2. Combustion Completeness

[16] Combustion completeness (*CC*), also called combustion fraction, is highly variable between different fires under different conditions even in similar vegetation types. However, *CC* for different ecosystem types can be loosely associated with fuel types, fuel loads, fuel configurations, and resulting combustion processes associated with those ecosystems. In this study, ecosystem types with similar characteristics are grouped together and assigned a *CC* based on the literature survey (Table 2). In some cases, we have used the averaged values for some of the ecosystem types because there are various field study results available for the same ecosystem type in the open literature, which give different numbers for *CC*. In the absence of the existence of a rigorous approach, we average the values for the different studies to give a representative value of *CC*.

2.3. Emission Factors

[17] Emission factors (*EFs*) are estimations of the mass of a given species emission relative to some measurement of total burned material. In this study, all *EFs* are given in terms of g species/kg dry matter. We use regional natural vegetation-based *EFs* (listed in Table 3), which are compiled from several publications for various regions and ecosystems. If the *EF* of a gas is available from many different sources, we use the average value of all available sources. In addition, if there is no regional *EF* value available, a global mean *EF* derived by *Andreae and Merlet* [2001] for different natural vegetation type is used.

2.4. GLOBSCAR and GBA Burnt Area Data Sets

[18] For the global burnt area we have used two of the latest open fire products recently made available. Both products are compilations of global monthly area burned during the year 2000 from two different remote sensing satellites. These two data sets are GLOBSCAR [*Simon et al.*, 2004] and GBA [*Grégoire et al.*, 2003; *Tansey et al.*, 2004]. Both data sets are freely distributed products and provide the monthly areas burned globally at 1 km $\times$ 1 km resolution.

[19] Both data sets have a number of shortcomings with respect to global biomass emission calculations. One of the common problems associated with both data sets is that they do not detect small burnt areas below 1 km^2. Previous emission inventory studies based on GLOBSCAR [*Hoelzemann et al.*, 2004], and GBA [*Ito and Penner*, 2004] data sets have used the ATSR active fire counts [*Arino and Plummer*, 2001] to account for small-undetected burnt area. These studies found very small increases (1–2%) in the area burned due to this correction [*Ito and Penner*, 2004; *Hoelzemann et al.*, 2004]. Moreover, earlier studies have also shown that the active fire products do not represent an unbiased sample of fire activity owing to poor sampling frequency and failure to detect small daytime fires [*Arino and Plummer*, 2001; *Schultz*, 2002; *Kasischke et al.*, 2003]. Therefore we do not apply this active fire count data correction in the current study.

[20] Two satellite data sets may also detect nonbiomass fires such as oil/gas flares and coal-mine fires. In this study, we prevent such problem by adding an algorithm in our calculation such that if burning occurs in the same pixel for four continuous months, we regard that burning as oil/gas flares or coal-mine fires and remove it from the calculation of total biomass burning emissions.

[21] The annual global burned areas used in this study for the year 2000 based on GLOBSCAR and GBA data sets were about 1.92 million km^2 and 3.49 million km^2, which are slightly lower than the area burned originally reported by the authors of GLOBSCAR (2.10 million km^2) [*Simon et al.*, 2004] and GBA (3.52 million km^2) [*Tansey et al.*, 2004] data sets, because we have excluded tundra and polar desert

Table 3. Emission Factors for Different Land Cover Types and Regions for Various Greenhouse Gas Emissions[a]

	CO	NO_x	NMHCs	CO2
	Tropical Evergreen			
Tropical America	122[b]	2.7[c]	8.4[d]	1580
Other Regions[e]	104	1.6	8.1	1580
	Tropical Deciduous			
Tropical America	79.2[f]	3.4[g]	8.1	1580
Other Regions[e]	104	3.0	8.1	1580
	Temperate Evergreen and Temperate Deciduous			
North America	98.5[h]	3.0	5.7	1569
Other Regions[e]	107.0	3.0	5.7	1569
	Boreal			
North America	115.0[i]	1.5[j]	5.7	1569
Former Soviet Union	175.7[k]	3.0	5.7	1569
Other Regions[e]	107	3.0	5.7	1569
	Savanna			
Tropical America	58.6[l]	2.3[d]	3.6[d]	1613
Tropical Africa	67.0[m]	3.1[n]	2.9[o]	1613
Oceanic	80[p]			1613
Other Regions[e]	65.0	3.9	3.4	1613
	Grassland/Pastureland/Shrubland/Desert			
Tropical Africa	62.4[q]	5.5[r]	3.6[s]	1613
Other Regions[e]	65.0	3.9	3.4	1613
	Cropland			
Tropical Africa[s]	117.0	2.8	5.0	1515
Other Regions[e]	92.0	2.5	7.0	1515

[a]Emission factors (EF), given in g species/kg dry matter.
[b]Average of *Ferek et al.* [1998], *Fearnside* [2000], and *Scholes and Andreae* [2000].
[c]Average of *Fearnside* [2000] and *Scholes and Andreae* [2000].
[d]*Scholes and Andreae* [2000].
[e]*Andreae and Merlet* [2001].
[f]Average of *Ward et al.* [1996], *Bertschi et al.* [2003], *Sinha et al.* [2003], and *Yokelson et al.* [2003].
[g]*Sinha et al.* [2003].
[h]Average of *Yokelson et al.* [1999] and *Friedli et al.* [2001].
[i]Average of *Cofer et al.* [1989, 1998], *Hegg et al.* [1990], *Radke et al.* [1991], *Susott et al.* [1991], *Yokelson et al.* [1997], *Goode et al.* [2000], *Bertschi et al.* [2003], and *French et al.* [2002].
[j]*Goode et al.* [2000].
[k]Average of *Cofer et al.* [1996] and *Bertschi et al.* [2003].
[l]Average of *Ward et al.* [1992] and *Ferek et al.* [1998].
[m]Average of *Cofer et al.* [1996], *Hao et al.* [1996], *Scholes et al.* [1996], *Sinha et al.* [2003], and *Yokelson et al.* [2003].
[n]Average of *Lacaux et al.* [1996], *Scholes et al.* [1996], *Sinha et al.* [2003], and *Yokelson et al.* [2003].
[o]Average of *Cofer et al.* [1996], *Ward et al.* [1996], *Korontzi et al.* [2003], and *Sinha et al.* [2003].
[p]*Hurst et al.* [1994a, 1994b] and *Shirai et al.* [2003].
[q]Average of *Scholes et al.* [1996], *Ward et al.* [1996], *Korontzi et al.* [2003], *Sinha et al.* [2003], and *Yokelson et al.* [2003].
[r]*Scholes et al.* [1996].
[s]*Saarnak et al.* [2003].

from burning owing to their negligible contributions in estimating biomass burning activities. As demonstrated by Figures 2a and 2b, the GBA results for most regions are substantially higher than GLOBSCAR results. This issue has been investigated in some detail by *Simon et al.* [2004], who compared the GLOBSCAR results to available statistics and other remote sensing products including ATSR-2 World Fire Atlas (WFA) [*Arino et al.,* 2001] and the GBA results; and by *Tansey et al.* [2004] who compared the GBA results to the available national burned statistics and

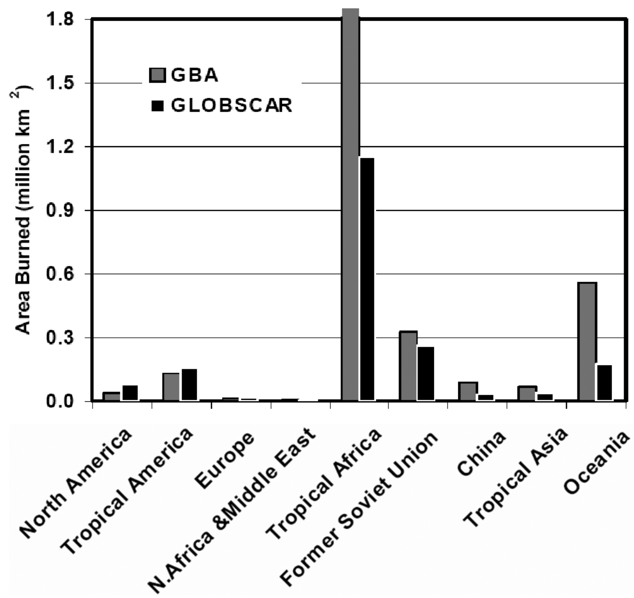

Figure 2a. Regional area burned (million km^2) from the open fires in the year 2000 based on GLOBSCAR and GBA data sets.

GLOBSCAR results for several regions. These previous comparisons help us to draw some conclusions about the potential and limitations of the GLOBSCAR and GBA results regionally. The most notable regional differences between the two data sets are seen in tropical Africa and Oceania, perhaps owing to known difficulties with GLOBSCAR detection of woodland and shrubland burning [*Simon et al.*, 2004]. The annual burnt area recorded by GLOBSCAR in North America and tropical America is higher than that recorded by GBA. While the authors of the GBA products acknowledge underdetection problems over North America, particularly in Canada [*Tansey et al.*, 2004], *Simon et al.* [2004] assert that the GBA product may be overreporting area burned owing to the mapping of scars from previous fires. GLOBSCAR results for tropical America are generally equal to what might be expected in this region [*Simon et al.*, 2004]. In the case of Tropical Asia and

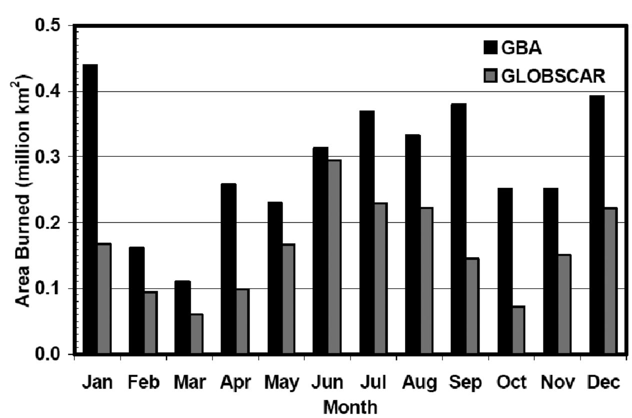

Figure 2b. Monthly area burned (million km^2) from the open fires for the year 2000 based on GLOBSCAR and GBA data sets.

China, the GLOBSCAR results for area burnt are about 50% lower than the GBA results. *Simon et al.* [2004] report that there were no validation data available for these regions. In Europe, North Africa, the Middle East, and the Former Soviet Union, burnt area based on both data sets are approximately the same. However, in the case of the Former Soviet Union, both the GLOBSCAR figures and GBA results are significantly larger than national reports and UN FAO statistics [*Simon et al.*, 2004; *Tansey et al.*, 2004].

2.5. Emissions From Land Clearing for Croplands

[22] To calculate the burning emissions due to changes in natural vegetation for croplands, a specified amount of biomass within a grid cell is subtracted from the three vegetation carbon pools (GV, NW, WTP) based on the relative proportions of the carbon contained in these reservoirs. A fraction of the released carbon is transferred to litter reservoirs as slash left on the ground. The rest is stored in burnable plant material pool (1-year pool) and wood and/or fuel product reservoirs (10-year, 100-year pools). The values of the fractions of total cleared vegetation burned (α), and used for wood and fuel products are taken from *Houghton and Hackler* [2001], which varies with land cover type and region. In order to avoid the double accounting of biomass burning due to land clearing data and satellite-based burning data within each 0.5 and 0.5 grid cell, the satellite data-based DM burned is revised by subtracting the DM burned owing to land clearing for croplands.

[23] The DM burned owing to land clearing for croplands is calculated on the basis of two sets of data for area cleared from croplands as implemented by *Jain and Yang* [2005]. The first set of data is primarily based on the deforestation rates compiled from national reports and remote sensing surveys from the United Nations FAO (Food and Agriculture Organization) Forest Resource Assessment (FRA) [*Houghton*, 2003; *Houghton and Hackler*, 1999, 2001] (HH hereafter) The HH data is available over the period 1765–2000. The other set of data is based on cropland statistics from the United Nations FAO [*Ramankutty and Foley*, 1998, 1999] (RF hereafter). The RF data set is available for the period 1765–1992. In order to calculate DM in the year 2000, we linearly extrapolated the RF data between 1992 and 2000 using the trend for the 1980s.

2.6. Emissions From Domestic Biofuel Burning

[24] Emissions from domestic biofuel burning in the year 2000 were calculated by multiplying the per capita fuel consumption rate by the total population. We use *Ludwig et al.*'s [2003] regional per capita consumption rates. The per capital domestic biofuel consumption rate covers all the activities associated with biofuel burning (e.g., cooking, heating, and charcoal making). The gridded 1990s world population from the United Nations Environmental Program (http://esa.un.org/unpp/) was projected to the year 2000 on the basis of the census population growth data from the United Nations. The estimated regional biofuel consumption was then distributed among the grids in each region by multiplying the population density per grid with the consumption rate for that region. Most fuelwood used in domestic biofuel burning comes from local ecosystems; as such, there is potential for errors due to double counting biomass usage. Double counting occurs when all biomass in a grid is used in the biomass burning calculation, and then fuelwood consumption of the same biomass occurs in the same grid. The assumption made in this study was that all fuelwood burned in a grid came from the biomass in the same grid. To minimize errors, fuelwood consumption was calculated per grid and then a check was done to see if burning occurred in that grid. If burning occurred within a grid cell, the biomass from fuelwood consumption was subtracted from the burned biomass load. On the basis of two burnt area data sets, about 3–5% of the fuelwood consumption was subtracted.

3. Results

3.1. Available Fuel Load

[25] Table 4 compares our ISAM model estimated *AFL* for various regions and across major ecosystem types with field experiment–based values available in the literature. It is important to recognize that there is no consistent global map of *AFL* available in the open literature. Most of the field experiment studies available in the literature are carried out on specific regions or a country using diverse methods. Therefore the uncertainty ranges for the available literature values are generally quite large (Table 4). Results from this study using tree density imagery as inputs to the terrestrial component of our ISAM indicate that the global and annual total AFL in the year 2000 for forest and nonforest biomes were 14,259 g/m^2 and 1073 g/m^2. The nonforest and forest biomes account for 10 and 90% of the global total AFL (687 Pg AFL/yr). Our modeling results indicate that the Former Soviet Union (FSU) forests contain the largest amount of AFL on the basis of density (18 kg/m^2), then North America (NA) (16 kg/m^2), North Africa and the Middle East (NAME)(15 kg/m^2), Tropical Africa (TAf) (13 kg/m^2), Tropical America (Tam) and Europe (EU) (12 kg/m^2), and Tropical Asia (TAs) (11 kg/m^2). All other regions produced less than 10 kg/m^2 AFL from forest biomes. In the case of nonforests, again FSU biomes contain the largest amount of AFL (1.9 kg/m^2), then EU (1.8 kg/m^2), TAs (1.4 kg/m^2) and, NA and China (1.0 kg/m^2); whereas other regions contain less than 1.0 kg/m^{2}n of nonforest AFL.

3.2. Dry Matter Burned

[26] Table 5 lists the ISAM estimated regional and total estimated global and annual mean dry matter (DM) burned (Tg DM/yr) based on various data sets for open fire biomass and domestic biofuel burning. The ISAM estimated dry matter burned, without land clearing for croplands, based on GLOBSCAR and GBA data sets for the year 2000 were 3099 Tg DM/yr and 4159 Tg DM/yr (Table 5). The differences in estimated DM burned for two data sets are due not only to the differences in the area burned, but also to the differences in fuel type burned (forests versus nonforest) from the two data sets described in section 2.4. On the basis of these two data sets, the TAf (1712–2654 TgDM/yr) region was the largest source of DM burned. The FSU was the second largest source of DM burned (586–670 Tg DM/yr). The estimated DM burned in the year 2000 for other regions were less than 500 Tg DM/yr (shown in Table 5). Our model estimated results are consistent with other modeling studies

Table 4. ISAM Estimated Available Fuel Load for Forest Ecosystems as Well as Totals for Forest and Nonforests Ecosystems and Regions for the Year 2000 Compared With Estimates Based on Field Measurements[a]

Region	Tropical	Temperate	Boreal	Total for Forest Ecosystem	Total for Nonforest Ecosystem
Tropical America	11,277 12,000–43,000[b] 6400–43,500[c]	13,586	n/a	12,297	600 710[d]
Tropical Africa	12,740	9800	n/a	12,738 9400–45,700[e]	756 72–478[f]
Tropical Asia	11,061	n/a	n/a	11,061	1370
North America	n/a	14,257 10,000–38,000[g]	16,803 8700–22,900[h] 19,200[i]	16,245	1037
Europe	18,333	12,371	10,819	11,520	1837
Former Soviet Union	n/a	14,054	18,347 5000[j]	18,018	1910
North Africa and Middle East	n/a	15,744	n/a	15,744	491
China	12,096	8172	7302	8109	1013
Oceania	11,471	11,941	n/a	11,766	653
Global total	**12,189**	**12,799**	**16,379**	**14,259**	**1073**

[a]Available fuel load in units of g/m^2.
[b]Brazil [*Ward et al.*, 1992; *Kauffman et al.*, 1995; *Guild et al.*, 1998].
[c]Brazil [*Stocks and Kauffman*, 1997].
[d]Brazilian savanna and grassland [*Ward et al.*, 1992; *Guild et al.*, 1998].
[e]Range values based on Guinean and Sudanian Savanna [*Pereira et al.*, 1999].
[f]South African and Zambian Savanna and Grassland [*Shea et al.*, 1996].
[g]Range values based on Oregon and Washington, U.S. regions [*Hobbs et al.*, 1996].
[h]Range values for Alaska Boreal regions taken from *Kasischke et al.* [2000]. The values were given in tC/ha, which were converted into total biomass by assuming 45% carbon per unit of total biomass.
[i]Surface biomass value for Alaska Boreal Forest taken from *Apps et al.* [1993].
[j]Siberia, Russia [*FIRESCAN Science Team*, 1996].

except for a few cases. For example, the ISAM estimated DM burned based on of GLOBSCAR and GBA data sets for most regions were substantially lower than *van der Werf et al.* [2003], which were averaged over the period 1998–2001. It is important to point out here that 1998 was an El Niño year with increased fire activity due to drought conditions, whereas the year 2000 was a La Niña year with less fire activity around the globe [*van der Werf et al.*, 2003]. This could be one of the reasons that the area burned estimates based on work by *van der Werf et al.* [2003], particularly in the tropics with the exception of the TAf for the GBA case, were higher than the ISAM estimates based on both (GBA and GLOBSCAR) data sets. The differences between the estimated DM of the ISAM and other studies might also be due to the differences in the *AFL* and *CC* values for different vegetation types, as well as different satellite platforms and different years of burning data sets. These other factors could be the reasons that the DM burned based on *van der Werf et al.* [2003] in TAf were lower than the ISAM estimates based on GBA data set, whereas the estimates were higher than the ISAM estimates based on GLOBSCAR. *Andreae and Merlet* [2001] also provided the global total value of DM burned for the late 1990s (5130 Tg DM/yr), which was originally estimated by J. A. Logan and R. Yevich from statistical ground-based measurement as summarized by *Lobert et al.* [1999]. The *Andreae and Merlet* [2001] value was higher than our estimated range of values (3099–4159 Tg DM/yr).

[27] Our modeling results suggest that land clearing for croplands in the year 2000 was the primary source of DM burned. The ISAM estimated total biomass burned based on two sets of satellite data for area burned (GLOBSCAR and GBA) and land clearing data (RF and HH) were 5221–7346 Tg DM/yr. The land clearing for cropland source contributed 2122–3187 Tg DM/yr (39 to 44% of total). The DM based on the RF data set was about 35% lower than that based on the HH data sets, mainly because the land clearing rates based on RF were lower than HH, particularly in the TAf. In general, our model results show the largest DM burned due to land clearing in tropical regions: TAs (1633–1925 Tg DM/yr), TAf (58–1013 Tg DM/yr), and TAm (99–201 TgDM/yr) (see Table 5). The data indicate that the land clearing activities were negligible in the nontropical regions. Therefore the estimated DM burned in these regions was either zero or small (Table 5).

[28] The estimated total annual and global DM burned due to domestic biofuel burning for the year 2000 was 3114 Tg DM/yr representing approximately 40–60% of the total DM burned due to biomass burning (see Table 5). Our estimates of DM burned due to domestic biofuel burning were higher than the estimates of *Andreae and Merlet* [2001], who reported 2701 Tg DM/yr. On the regional scale, the largest biofuel consumption occurred in TAs (940 Tg DM/yr), China (686 Tg DM/yr), and TAf (559 Tg DM/yr). Our estimated domestic biofuel DM burned for these regions were consistent with recent estimates by *Yevich and Logan* [2003].

3.3. Emissions From Open Fire Biomass and Domestic Biofuel Burning

3.3.1. Annual Global Total Emissions

[29] Our model estimated reactive GHG and CO_2 emissions for the year 2000 from open fire biomass and domestic biofuel burning sources are summarized in Table 6. Overall, our modeled global total emissions due to biomass burning for the 2000 were 438–568 Tg CO/yr,

Table 5. Comparison of the Estimated Dry Matter Burned for the Year 2000 With Other Model-Based Studies[a]

	Open Fire Biomass Burning						Domestic Biofuel Burning	
	Without Land Clearing			Land Clearing				
Region	ISAM-GLOBSCAR	ISAM- GBA	Other Studies	ISAM- RF	ISAM- HH	Total ISAM	ISAM-Biofuel	Other Studies
Tropical America	181	145	177–187[b] 1510[c]	99	201	244–382 1570[d]	231	328[e] 120[d]
Tropical Africa	1712	2654	1824–2705[b] 2170[c]	58	1013	1770–3667 704–2168[f] 2320[d]	559	536[e] 180[d]
Tropical Asia	88	148	124–143[b] 770[c]	1633	1925	1721–2073 880[d]	940	930[e] 320[d]
North America	405	164	840[c]	47	0	164–452	231	
Europe	24	28		48	0	28–72	76	
Former Soviet Union	586	670		159	0	586–829	96	
North Africa and Middle East	12	9		28	7	16–40	255	
China	39	138		42	0	39–180	686	677[e]
Oceania	51	201	340[c] 208–287[b]	8	40	59–241 319[d]	39	1[d]
Global total	3099	4159	5630[c] 2794–3814[b] 5130[g]	2122	3187	5221–7346	3114	2701[g]

[a]Dry matter burned in units of Tg DM/yr.
[b]Year 2000 using the GBA global area burned data [*Ito and Penner*, 2004].
[c]Average for the period 1998–2001 using the TRMM satellite data for the region between 38°N and 38°S [*van der Werf et al.*, 2003].
[d]For late 1970s [*Hao and Liu*, 1994].
[e]Year 1995 derived from statistical ground-based estimates [*Yevich and Logan*, 2003].
[f]During 1985–1991 [*Barbosa et al.*, 1999].
[g]Late 1990s [*Andreae and Merlet*, 2001].

11–16 Tg NO_x/yr (as NO), 29–40 Tg NMHCs/yr, and 6564–9093 Tg CO_2/yr; whereas other modeling study estimates ranged between 171––429 Tg CO, 16–24 Tg NO_x (as NO), 9–29 Tg NMHCs and 4477–7864 Tg CO_2 [*Andreae and Merlet*, 2001; *Duncan et al.*, 2003; *Ito and Penner*, 2004; *van der Werf et al.*, 2003, 2004; *Hoelzemann et al.*, 2004]. It is important to note that our model estimated values for most of the cases are higher than those estimated

Table 6. Comparison of ISAM Estimated Open Fire Biomass and Domestic Biofuel Burning Emissions for CO, NO_x (as NO), NMHCs, and CO_2 for the Year 2000 With Other Model-Based Emission Estimates[a]

	CO	NO_x	NMHCs	CO_2
	ISAM-Biomass Burning			
This study: without land clearing (GLOBSCAR – GBA)	320.6–406.7	8.5–12.2	21.1–27.8	4888–6570
This study: land clearing (RF – HH)	112.1–163.0	2.2–3.6	8.1–12.1	1676–2523
This study total	437.7–567.7	10.7–15.8	29.2–39.9	6564–9093[b]
Other studies				
Andreae and Merlet [2001][c]	423.4	16.5	29.4	7864
Ito and Penner [2004][d]	263.0–421.0		18.7–27.1	4477–5982
van der Werf et al. [2003][e]				7634
Hoelzemann et al. [2004][f]	271	24.3	8.8	5716
van der Werf et al. [2004][g]	171–408			
Duncan et al. [2003][h]	429			
	Biofuel Burning			
This study	242.8	3.4	22.7	4825[b]
Other studies				
Andreae and Merlet [2001][c]	209	2.9	19.6	4187
Ito and Penner [2004][d]	232	2.2	19.3	3853
Yevich and Logan [2003][i]	156	4.0		2688

[a]Emissions are in units of Tg Gas/yr. Open fire biomass burning emissions are calculated on the basis of GLOBSCAR and GBA fires, and HH and RF land clearing for cropland data sets, whereas domestic biofuel burning emissions are calculated on the basis of the regional per capita biofuel consumption rates.
[b]The total carbon lost from cropland clearing and biofuels (6501–7348 TgCO2/yr) is reasonably close to *Houghton*'s [2003] estimate of the amount of carbon released as a result of all clearing practices + fuelwood use (TgCO2/yr for the 1990s) (R. A. Houghton, personal communication, 2005).
[c]Late 1990s use global biomass burning inventory estimates. Emissions from charcoal are excluded.
[d]Year 2000 uses global GBA burned data.
[e]Average for the period 1998–2001 uses the satellite TRMM data between 38°N and 38°S.
[f]Year 2000 uses global GLOBSCAR open fire burned data.
[g]Year 2000 uses the satellite TRMM data and an inverse analysis of atmospheric CO anomalies between 38°N and 38°S.
[h]Year 1999 uses global ATSR and AVHRR fire-count data.
[i]Year 1995 is derived from statistical ground-based estimates.

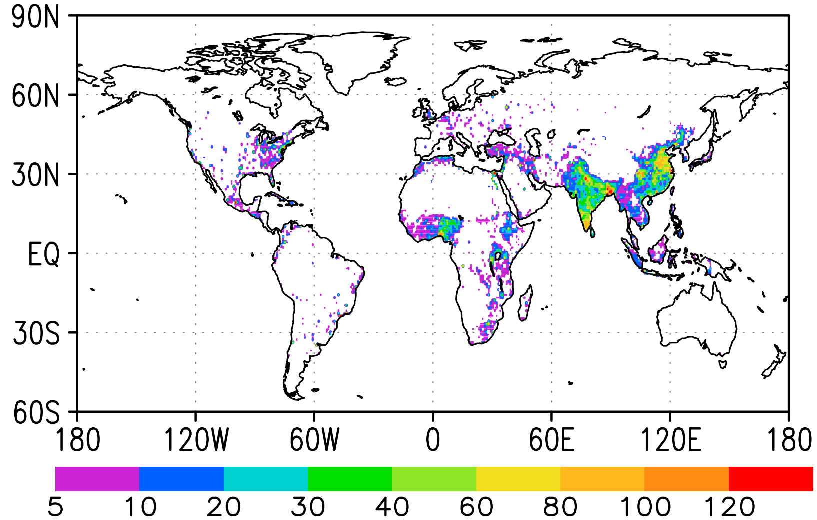

Figure 3. ISAM estimated total annual CO emissions (Gg CO) associated with domestic biofuel burning for the year 2000.

by other studies. However, our results without land clearing effects are in much better agreement with other modeling results. These results clearly suggest that land clearing has a substantial influence on the emissions of various tracers studied here. On the basis of our model results, the land clearing source constituted about 25–28% (CO), 20–23% (NO), 28–30% (NMHCs), and 25–27% (CO_2) of the total open fire biomass burning emissions of these gases.

[30] Figure 3 and Table 6 show the model estimated global distribution of CO emissions for the domestic biofuel burning in the year 2000. Our model estimated global rates of 243 Tg CO/yr, 3 Tg NO_x/yr (as NO), 23 Tg NMHCs/yr, and 4825 Tg CO_2/yr were consistent with those of *Andreae and Merlet* [2001] and *Ito and Penner* [2004]. *Yevich and Logan* [2003] estimated domestic biofuel emissions of 156 Tg CO, 4.0 Tg NO_x (as NO) and 2688 Tg CO_2 for the developing world (tropical Asia, tropical America, tropical Africa, and China). As compared to *Yevich and Logan* [2003], our model estimated emissions for the developing world are somewhat higher in the case of CO (188 Tg CO) and CO_2 (3745 Tg CO_2), but lower in the case of NO_x (2.7 Tg NO).

3.3.2. Spatial and Seasonal Distributions for Open Fire Emissions

[31] Spatial distributions of biomass-burning emissions are exclusively tied to spatial detections of burned area by GLOBSCAR and GBA data sets. Large emissions occur in areas where heavy burning happens. This feature is well illustrated in Figure 4, which displays the spatial distributions of CO emissions associated with two fire data sets for the months of March, June, September, and December of the year 2000 at $0.5° \times 0.5°$ spatial resolution. The emission estimates based on two burned products show roughly similar seasonal distributions throughout the year, but their extent is lower in most of the regions when using the GLOBSCAR data set. All of these differences are further discussed below by comparing seasonal variations in CO emissions for global total and nine regions based on two area burned data sets (Figure 5).

[32] It is important to recognize that the seasonal patterns of global total emissions for the CO based on two data sets are approximately the same, except for the month of June when the emissions based on GBA data were decreasing, whereas emissions based on GLOBSCAR were rapidly peaking. The most notable seasonal differences in CO emissions based on two burned area products exist in North America with much larger emission estimates based on GLOBSCAR in the month of June of 2000 than emission estimates based on GBA. According to *Hoelzemann et al.* [2004], the June maximum in the North American burned area in GLOBSCAR is a detection error related to the misclassification of bare soils.

[33] In Europe, the emissions based on GLOBSCAR are substantially higher during the month of April, May, and August compared to emissions based on GBA; in the Former Soviet Union, the emission results of GBA in the months of April and May are higher than the results of GLOBSCAR; and in Tropical America, no consistent seasonal patterns are found between the two data sets. The regions with the most similar emission patterns based on both data sets are Tropical Africa, Tropical Asia, and, to a lesser extent, North Africa and the Middle East, China, and Oceania.

4. Discussion and Conclusions

[34] The open fire biomass and domestic biofuel burning algorithms have been incorporated within the framework of ISAM to estimate the emissions of reactive GHGs (CO, NO_x, and NMHCs) and CO_2. We applied the ISAM framework along with two recently available satellite data sets (GLOBSCAR and GBA) for area burned, satellite-derived tree density data, two sets of land clearing for cropland data sets (RF and HH data sets), and regional biofuel consumption data to estimate the AFL, DM burned, and emissions for the reactive GHGs and CO_2 for the year 2000.

[35] Our model estimated global AFL for forest and nonforest biomes for the year 2000 are 14,259 g/m^2 and

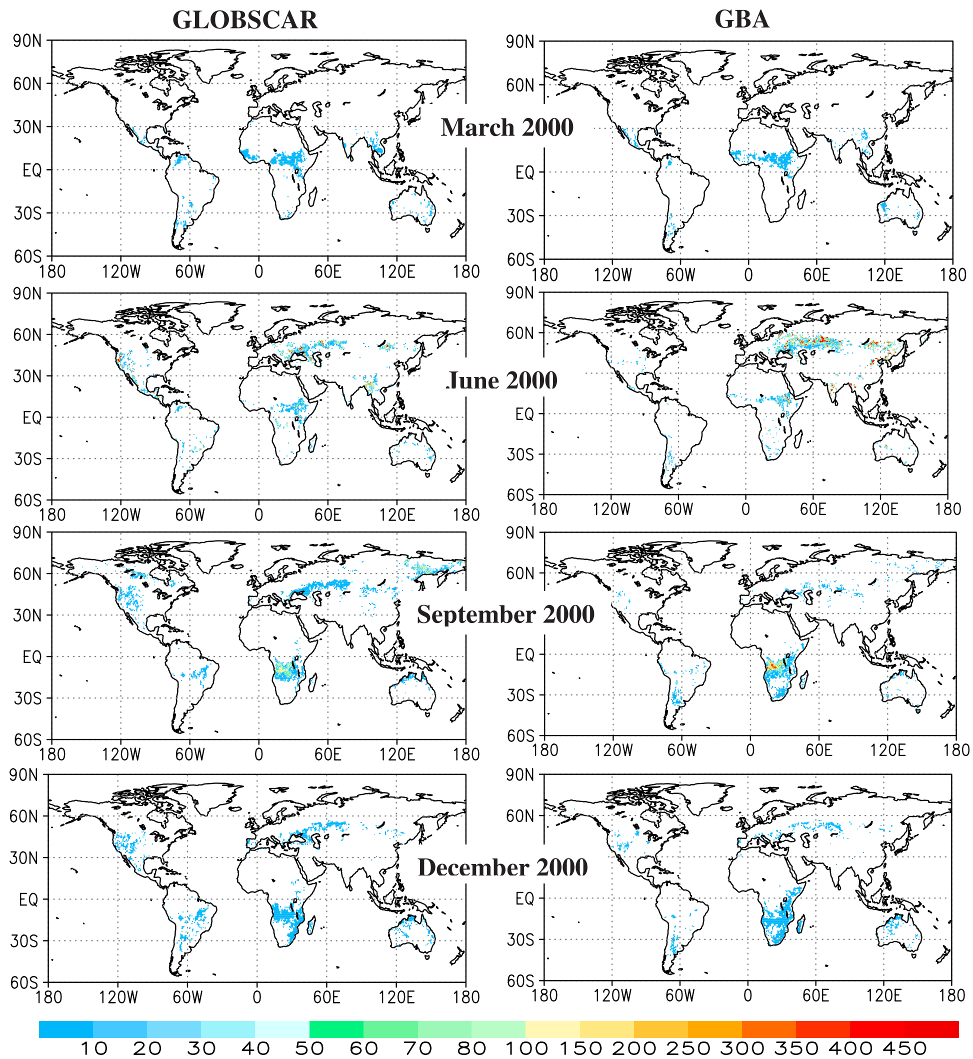

Figure 4. ISAM estimated monthly CO emissions (Gg CO) associated with GLOBSCAR and GBA open fires data sets for the months of March, June, September, and December of the year 2000.

1076 g/m^2. Regional ISAM estimates for AFL are well within the range of available ground-based measurements. However, the uncertainty ranges for the available literature values are generally quite large mainly because estimates are carried out on a very specific region or a country using diverse methods.

[36] Using the two sets of data each for open fire area burned (GLOBSCAR and GBA) and land clearing for croplands for the year 2000, the estimated global total DM burned and the resultant release of various gases considered here ranges between 5221–7346 Tg DM/yr; and 6564–9093 Tg CO_2/yr, 438–568 Tg CO/yr, 11–16 Tg NO_x/yr, and 29–40 Tg NMHCs/yr. An important conclusion of this research is that land clearing for croplands has a profound impact on the amount of biomass burned and the resultant emissions of reactive GHGs and CO_2. Our model results indicate that such activities could have contributed up to 43% to the global total biomass burned; and 27% (CO_2), 28% (CO), 23% (NO), and 30% (NMHCs) of the total biomass burning emissions of these gases. It is also important to recognize that our model estimated results of biomass burning based only on the GLOBSCAR and GBA data sets (i.e., without taking into account the land clearing effects) are consistent with other model studies that estimate the emissions using the same area burned data sets and a similar modeling approach. However, our estimated values for without land clearing sources are substantially lower than ground measurement–based or inverse modeling-based estimates [*Arellano et al.*, 2004; *Carmichael et al.*, 2003; *van der Werf et al.*, 2004]. For example, our model estimated CO emissions without land clearing sources in the South and South East Asia (SSEA) region were 9–15 Tg CO/yr, significantly smaller than most recent inverse modeling–based estimates of 95–120 Tg CO/yr for biomass burning [*Arellano et al.*, 2004]. However, after accounting for land clearing effects, our estimated emissions for SSEA region were 93–115 Tg CO/yr, consistent with values estimated by *Arellano et al.* [2004].

[37] Our model results indicate that the burning of domestic biofuels also provide major sources of reactive GHGs and CO_2. The estimated global source strengths

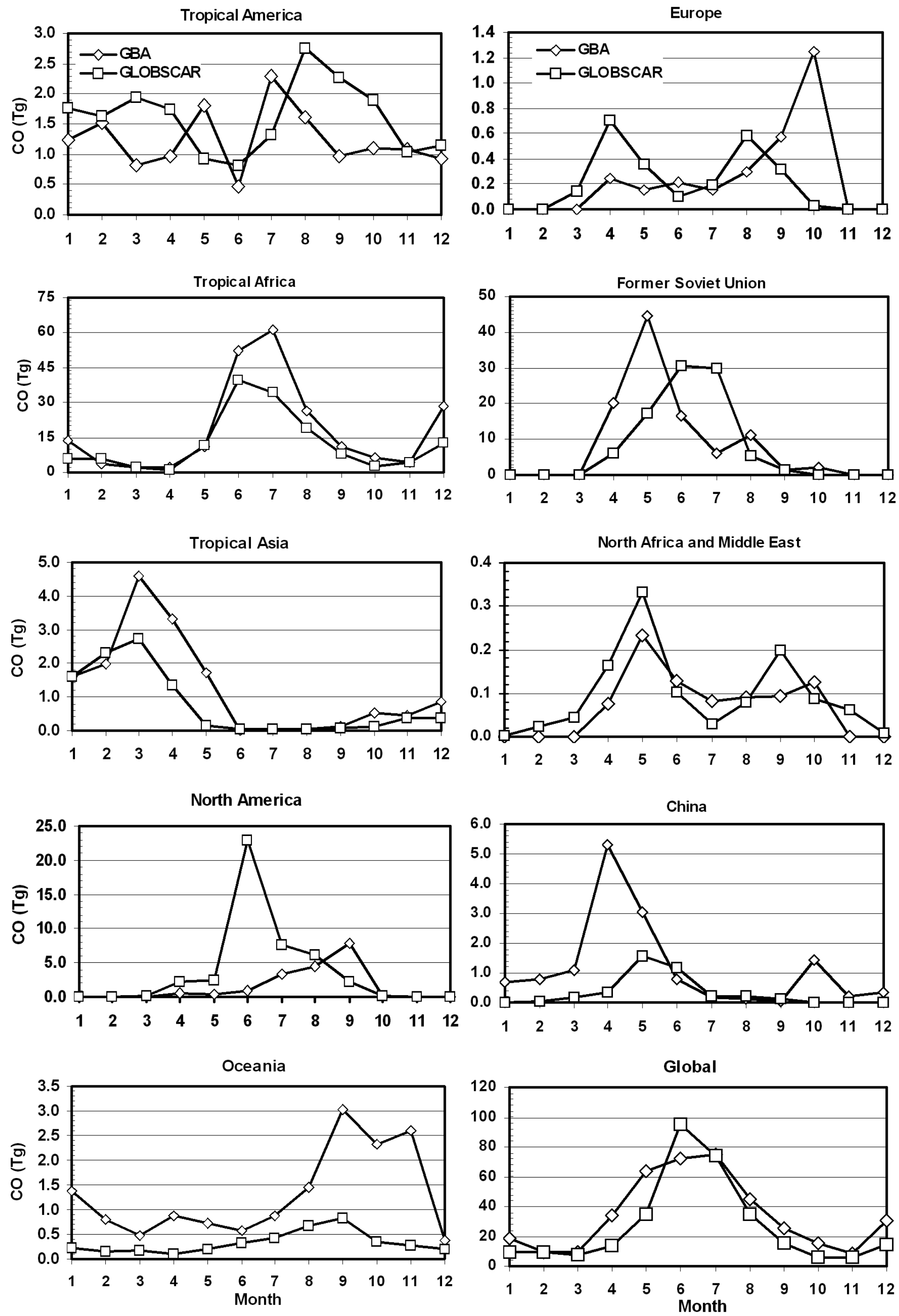

Figure 5. Comparisons of the monthly variations for the year 2000 in CO emissions based on the GLOBSCAR and GBA open fire data sets. The comparisons are shown for the global total and nine regions shown in Figure 1.

for domestic biofuel burning in the year 2000 are on the order of 243 Tg CO/yr, 3.4 Tg NO_x/yr, 23 Tg NMHCs/yr, and 4,825 Tg CO_2/yr. More than 90% of these emissions are in tropical regions (Asia, Africa, America, and China).

[38] There are undoubtedly limitations in the modeling method used here to estimate open fire biomass and domestic biofuel burning emissions due to uncertainties associated with the various input variables used. Given the high correlation between the emissions and area burnt, it is most likely that the uncertainties in the calculated open fire biomass burning emissions stem primarily from the area burned data for which we rely on the two satellite measurements of burnt area. We believe that large uncertainties in the two sets of area burned data merits comprehensive investigation. Similar conclusions have been made through review efforts of the Global Observations of Forest Cover (GOFC) project and the International Geosphere-Biosphere Program (IGBP) [*Kasischke and Penner*, 2004]. With

regards to the land clearing emissions, we believe that there is a large uncertainty in both sets of data used here (HH and RF), which merits further investigation with ground and satellite-based measurements. In conjunction with such efforts, local and global land cover changes could also be measured to validate the performance of terrestrial ecosystem models.

[39] Another potential area of uncertainty is the *AFL* for which we rely on satellite based land cover information in our terrestrial model. The estimates of *AFL* are mainly a function of aboveground carbon content, which we estimated using our dynamic terrestrial ecosystem component of the ISAM. The incorporation of a 0.5° spatially resolved terrestrial model provides the essential capability for investigating potential changes in open fire biomass-burning emissions due to changes in climate and land-use practices. We also used forest inventory data to assess the quantity of forest resources at the 1 km^2 resolution. The resolution of the forest density data was consistent with the area burned data from two burnt products used in this study. Nevertheless, uncertainties in our model results could arise from ecosystem classification. Moreover, our model estimated AFL might be overestimated because we did not account for the fires at the spin-up state (year 1765) and over the period 1766–1999 owing to limited data information. Fires over the historical time may have lowered the biomass of forests, grasslands and savanna [*Houghton et al.*, 2001]. We have also not accounted for under-story fires (such as boreal peatland and Indonesian peatland fires), because GLOBSCAR and GBA data products were unable to detect such small-sized fires [*Simon et al.*, 2004; *Tansey et al.*, 2004].

[40] The *CC* of the actual biomass burned is also a key in accurately determining emissions. Here *CC* was assumed as a function of ecosystem type, but it could also depend on the combustion process and fuel moisture content. The uncertainty level is very difficult to quantify for *CC* because combustion processes are heterogeneous in nature and vary widely under different combustion conditions. There are studies that have shown statistically significant links between fuel moisture and *CC*, especially in savanna ecosystems [*Hoffa et al.*, 1999]. Alternatively, some studies are starting to base their *CC* estimates on fuel composition types as opposed to ecosystem types. For example, *CC*s are assigned to grasses/leaves, twigs, branches, and logs. The proportion of carbon that is stored in grasses/leaves, twigs, branches, or logs is then determined by ecosystem type, soil types, and weather factors. In the future this might be a more accurate way to assess *CC* for biomass burning studies, especially if coupled with fuel moisture models.

[41] Further uncertainties in calculations of open fire biomass burning emissions is garnered by the emission factors (*EF*) from biomass burning. Considerable progress has recently been made to determine accurate values of *EF*. In particular, *Andreae and Merlet* [2001] have critically evaluated the presently available data and integrated it into a consistent format. In this study, we assigned biome specific *EF*s where possible for any gaps in the averaged values from *Andreae and Merlet* [2001]. In spite of recent progress, gaps remain in the evaluation of *EFs*, particularly with respect to the estimates of emissions as a function of space, time and type of combustion. For example, CO emission factors are low during the flaming combustion stage but significantly higher in the smoldering stage [*Yokelson et al.*, 1997; *Kasischke and Bruhwiler*, 2003]. Explicit representation of these two combustion stages would be desirable, but are not currently available because of limited data. The uncertainty associated with this parameterization and a host of other standard and necessary simplifications is difficult to assess. Second, the amount and accuracy of *EF* and *CC* data is not equally represented among ecosystems. Savanna and grasslands have received the majority of attention, and as such have some of the most refined data. Other ecosystems such as boreal forests are understudied and as such represent a large area of uncertainty. Future study of *CC*s and *EF*s in other ecosystems are warranted to increase the accuracy of our current data.

[42] The uncertainty in estimate of domestic biofuel emissions is also quite large owing to uncertainties associated with various input variables used. As also suggested by *Ludwig et al.* [2003], quantification of the annual global domestic biofuel consumption is the major constraint in a more accurate estimate of emissions from domestic biofuel burning. Improved knowledge of this consumption should be an objective for future research.

[43] In conclusion, the ISAM modeling framework presented here is quite sophisticated for estimating the emissions of reactive and nonreactive GHG emissions due to open fire biomass and domestic biofuel burning. It is also flexible enough to incorporate the latest data and experimental results as they become available in the open literature. A fully coupled ISAM could potentially provide an internally consistent framework to investigate the impact of climate change on open fire biomass and domestic biofuel emissions, chemistry, and ecosystems, as well as feedbacks of changing emissions and chemistry to future climate. We plan to update the ISAM results with time and make them available on the ISAM web site (http://isam.atmos.uiuc.edu/).

[44] **Acknowledgments.** We thank James T. Randerson and two anonymous reviewers for providing valuable comments on the earlier version of this manuscript. This research was supported in part by the Office of Science (BER), U.S. Department of Energy (DOE-DE-FG02-01ER63463).

References

Andreae, M. O., and P. Merlet (2001), Emission of trace gases and aerosols from biomass burning, *Global Biogeochem. Cycles*, *15*(4), 955–966.

Apps, M. J., W. A. Kurz, R. J. Luxmoore, L. O. Nilsson, R. A. Sedjo, R. Schmidt, L. G. Simpson, and T. S. Vinson (1993), Boreal forests and tundra, *Water Air Soil Pollut.*, *70*, 39–53.

Arellano, F. A., P. S. Kasibhatla, L. Giglio, G. R. van der Werf, and J. Randerson (2004), Top-down estimates of global CO sources using MOPITT measurements, *Geophys. Res. Lett.*, *31*, L01104, doi:10.1029/2003GL018609.

Arino, O., and S. Plummer (Eds.) (2001), *Along Track Scanning Radiometer World Fire Atlas: Validation of the 1997–98 Active Fire Product*, Eur. Space Res. Inst., Eur. Space Agency, Frascati, Italy.

Barbosa, P. M., D. Stroppiana, J.-M. Grégoire, and J. M. C. Pereira (1999), An assessment of vegetation fire in Africa (1981–1991): Burned areas, burned biomass, and atmospheric emissions, *Global Biogeochem. Cycles*, *13*(4), 933–950.

Bertschi, I., R. J. Yokelson, D. E. Ward, R. E. Babbitt, R. A. Susott, J. G. Goode, and W. M. Hao (2003), Trace gas and particle emissions from fires in large diameter and belowground biomass fuels, *J. Geophys. Res.*, *108*(D13), 8472, doi:10.1029/2002JD002100.

Carmichael, G. R., et al. (2003), Evaluating regional emissions estimates using the TRACE-P observations, *J. Geophys. Res.*, *108*(D21), 8810, doi:10.1029/2002JD003116.

Cochrane, M. A., A. Alencar, M. D. Schulze, C. M. Souza Jr., D. C. Nepstad, P. Lefebvre, and E. A. Davidson (1999), Positive feedbacks in the fire dynamic of closed canopy tropical forests, *Science*, *284*, 1832–1835.

Cofer, W. R., III, J. S. Levine, D. I. Sebacher, E. L. Winstead, P. J. Riggan, B. J. Stocks, J. A. Brass, V. G. Ambrosia, and V. J. Boston (1989), Trace gas emissions from chaparral and boreal forest fires, *J. Geophys. Res.*, *94*(D2), 2255–2259.

Cofer, W. R., III, J. S. Levine, E. L. Winstead, D. R. Cahoon, D. I. Sebacher, J. P. Pinto, and B. J. Stocks (1996), Source composition of trace gases released during African savanna fires, *J. Geophys. Res.*, *101*(D19), 23,597–23,602.

Cofer, W. R., III, E. L. Winstead, B. J. Stocks, J. G. Goldammer, and D. R. Cahoon (1998), Crown fire emissions of CO_2, CO, H_2, CH_4, and TNMHC from a dense jack pine boreal forest fire, *Geophys. Res. Lett.*, *25*(21), 3919–3922.

Crutzen, P. J., and M. O. Andreae (1990), Biomass burning in the tropics: Impact on atmospheric chemistry and biogeochemical cycles, *Science*, *250*, 1669–1678.

Daniel, J. S., and S. Solomon (1998), On the climate forcing of carbon monoxide, *J. Geophys. Res.*, *103*(D11), 13,249–13,260.

Duncan, B. N., R. V. Randall, A. C. Staudt, R. Yevich, and J. A. Logan (2003), Interannual and seasonal variability of biomass burning emissions constrained by satellite observations, *J. Geophys. Res.*, *108*(D2), 4100, doi:10.1029/2002JD002378.

Fearnside, P. (2000), Global warming and tropical land-use change: Greenhouse gas emissions from biomass burning, decomposition and soils in forest conversion, shifting cultivation and secondary vegetation, *Clim. Change*, *46*, 115–158.

Ferek, R. J., J. S. Reid, P. V. Hobbs, D. R. Blake, and C. Liousse (1998), Emission factors of hydrocarbons, halocarbons, trace gases, and particles from biomass burning in Brazil, *J. Geophys. Res.*, *103*(24), 32,107–32,118.

FIRESCAN Science Team (1996), Fire in ecosystems of boreal Eurasia: The Borel Forest Island Fire Experiment Fire Research Campaign Asia-North (FIRESCAN), in *Biomass Burning and Global Change*, vol. 1, edited by J. S. Levine, pp. 848–873, MIT Press, Cambridge, Mass.

French, N. H. F., E. S. Kasischke, and D. G. Williams (2002), Variability in the emission of carbon-based trace gases from wildfire in the Alaskan boreal forest, *J. Geophys. Res.*, *107*, 8151, doi:10.1029/2001JD000480. [printed *108*(D1), 2003].

Friedli, H., H. Lötscher, H. Oeschger, U. Siegenthaler, and B. Stauffer (1986), Ice core record of $^{13}C/^{12}C$ ratio of atmospheric CO_2 in the past two centuries, *Nature*, *324*, 237–238.

Friedli, H. R., E. Atlas, V. R. Stroud, L. Giovanni, T. Campos, and L. F. Radke (2001), Volatile organic trace gases emitted from North American wildfires, *Global Biogeochem. Cycles*, *15*(2), 435–452.

Fuglestvedt, J. S., I. S. A. Isaksen, and W.-C. Wang (1996), Estimates of indirect global warming potentials fro CH_4, CO, and NO_x, *Clim. Change*, *34*, 405–437.

Galanter, M., H. Levy II, and G. R. Carmichael (2000), Impacts of biomass burning on tropospheric CO, NO_x, and O3, *J. Geophys. Res.*, *105*(D5), 6633–6653.

Goldammer, J. G., and R. W. Mutch (2001), Global forest fire assessment 1990–2000, *Working Pap. 55*, FAO For. Resour. Program, Rome.

Goode, J. G., R. J. Yokelson, D. E. Ward, R. A. Susott, R. E. Babbitt, M. A. Davies, and W. M. Hao (2000), Measurements of excess O_3, CO_2, CO, CH_4, C_2H_4, C_2H_2, HCN, NO, NH_3, HCOOH, CH_3COOH, HCHO, and CH_3OH in 1997 Alaskan biomass burning plumes by airborne Fourier transform infrared spectroscopy (AFTIR), *J. Geophys. Res.*, *105*(D17), 22,147–22,166.

Grégoire, J.-M., K. Tansey, and J. M. N. Silva (2003), The GBA2000 initiative: Developing a global burned area database from SPOT-VEGETATION imagery, *Int. J. Remote Sens.*, *24*, 1369–1376.

Guild, L. S., J. B. Kauffman, L. J. Ellingson, D. L. Cummings, E. A. Castro, R. E. Babbitt, and D. E. Ward (1998), Dynamics associated with total aboveground biomass C, nutrient pools, and biomass burning of primary forest and pasture in Rondônia, Brazil during SCAR-B, *J. Geophys. Res.*, *103*(D24), 32,091–32,100.

Hao, W. M., and M.-H. Liu (1994), Spatial and temporal distribution of tropical biomass burning, *Global Biogeochem. Cycles*, *8*(4), 495–504.

Hao, W. M., M.-H. Liu, and P. J. Crutzen (1990), Estimates of annual and regional releases of CO_2 and other trace gases to the atmosphere from fires in the tropics, based on the FAO statistics 47 for the period 1975–1980, in *Fire in the Tropical Biota: Ecosystem Processes and Global Challenges*, edited by J. G. Goldammer, pp. 440-462, Springer, New York.

Hao, W. M., D. E. Ward, G. Olbu, and S. P. Baker (1996), Emissions of CO_2, CO, and hydrocarbons from fires in diverse African savanna ecosystems, *J. Geophys. Res.*, *101*(D19), 23,577–23,584.

Haxeltine, A., and I. C. Prentice (1996), BIOME3: An equilibrium terrestrial biosphere model based on ecophysiological constraints, resource availability, and competition among plant functional types, *Global Biogeochem. Cycles*, *10*(4), 693–709.

Hayhoe, K., A. Jain, H. S. Kheshgi, and D. Wuebbles (2000), Contribution of CH_4 to multi-gas reduction targets: The impact of atmospheric chemistry on GWPs, in *Non-CO_2 Greenhouse Gases: Scientific Understanding, Control and Implementation*, edited by J. van Ham, pp. 425–432, Springer, New York.

Hegg, D. A., L. F. Radke, and P. V. Hobbs (1990), Emissions of some trace gases from biomass fires, *J. Geophys. Res.*, *95*(D5), 5669–5675.

Hély, C., S. Alleaume, R. J. Swap, H. H. Shugart, and C. O. Justice (2003), SAFARI-2000 characteristics of fuels, fire behavior, combustion completeness, and emissions from experimental burns in infertile grass savannas in western Zambia, *J. Arid Environ.*, *54*, 381–394.

Hobbs, P. V., J. S. Reid, J. A. Herring, J. D. Nance, R. E. Weiss, J. L. Ross, D. A. Hegg, R. D. Ottmar, and C. Liousse (1996), Particle and trace-gas measurements in smoke from prescribed burns of forest products in the Pacific Northwest, in *Biomass Burning and Global Change*, vol. 1, edited by J. S. Levine, pp. 697–715, MIT Press, Cambridge, Mass.

Hoelzemann, J. J., M. G. Schultz, G. P. Brasseur, C. Granier, and M. Simon (2004), Global Wildland Fire Emission Model (GWEM): Evaluating the use of global area burnt satellite data, *J. Geophys. Res.*, *109*, D14S04, doi:10.1029/2003JD003666.

Hoffa, E. A., D. E. Ward, G. J. Olbu, and S. P. Baker (1999), Emissions of CO_2, CO, and hydrocarbons from fires in diverse African savanna ecosystems, *J. Geophys. Res.*, *104*(D11), 13,841–13,853.

Houghton, R. A. (2003), Revised estimates of the annual net flux of carbon to the atmosphere from changes in land use 1850–2000, *Tellus, Ser. B*, *55*, 378–390.

Houghton, R. A., and J. L. Hackler (1999), Emissions of carbon from forestry and land-use change in tropical Asia, *Global Change Biol.*, *5*, 481–492.

Houghton, R. A., and J. L. Hackler (2001), Carbon flux to the atmosphere from land-use changes: 1850 to 1990, *NDP-050/R1*, 86 pp., Carbon Dioxide Inf. Anal. Cent., Oak Ridge Natl. Lab., U.S. Dep. of Energy, Oak Ridge, Tenn. (Available at http://cdiac.esd.ornl.gov/ndps/ndp050.html)

Houghton, R. A., J. L. Hackler, and K. T. Lawrence (2001), Changes in terrestrial carbon storage in the United States: 2. The role of fire management, *Global Ecol. Biogeogr.*, *9*, 145–170.

Hurst, D. F., D. W. T. Griffith, and G. D. Cook (1994a), Trace gas emissions and biomass burning in tropical Australian savannas, *J. Geophys. Res.*, *99*(D8), 16,441–16,456.

Hurst, D. F., D. W. T. Griffith, J. N. Carras, D. J. Williams, and P. J. Fraser (1994b), Measurements of trace gas emitted by Australian savanna fires during the 1990 dry season, *J. Atmos. Chem.*, *18*, 33–56.

Ito, A., and J. E. Penner (2004), Global estimates of biomass burning emissions based on satellite imagery for the year 2000, *J. Geophys. Res.*, *109*, D14S05, doi:10.1029/2003JD004423.

Jain, A. K., and X. Yang (2005), Modeling the effects of two different land cover change data sets on the carbon stocks of plants and soils in concert with CO_2 and climate change, *Global Biogeochem. Cycles*, *19*, GB2015, doi:10.1029/2004GB002349.

Kasischke, E., and L. Bruhwiler (2003), Emissions of carbon dioxide, carbon monoxide, and methane from boreal forest fires in 1998, *J. Geophys. Res.*, *108*(D1), 8146, doi:10.1029/2001JD000461.

Kasischke, E. S., and J. E. Penner (2004), Improving global estimates of atmospheric emissions from biomass burning, *J. Geophys. Res.*, *109*, D14S01, doi:10.1029/2004JD004972.

Kasischke, E. S., K. P. O'Neill, N. H. F. French, and L. L. Bourgeau-Chavez (2000), Controls on patterns of biomass burning in Alaskan boreal forests, in *Fire, Climate Change, and Carbon Cycling in the North American Boreal Forest*, edited by E. S. Kasischke and B. J. Stocks, pp. 173–196, Springer, New York.

Kasischke, E. S., J. H. Hewson, B. J. Stocks, G. van der Werf, and J. T. Randerson (2003), The use of ATSR active fire counts for estimating relative patterns of biomass burning—A study from the boreal forest region, *Geophys. Res. Lett.*, *30*(18), 1969, doi:10.1029/2003GL017859.

Kauffman, J. B., D. L. Cummings, D. E. Ward, and R. Babbitt (1995), Fire in the Brazilian Amazon: Biomass, nutrient pools, and losses in slashed primary forest, *Oecologia*, *104*, 397–408.

Keeley, J. E., C. J. Fotheringham, and M. Morais (1999), Reexamining fire suppression impacts on Brushland fire regimes, *Science*, *284*, 1829–1832.

Keeling, C. D., and T. P. Whorf (2000), Atmospheric CO_2 records from sites in the SIO air sampling network, in *Trends: A Compendium of Data on Global Change*, Carbon Dioxide Inf. Anal. Cent., Oak Ridge Natl. Lab., Oak Ridge, Tenn.

Kheshgi, H. S., and A. K. Jain (1999), Reduction of the atmospheric concentration of methane as a strategic response option to global climate change, in *Greenhouse Gas Control Technologies*, edited by P. Reimer, B. Eliasson, and A. Wakaun, pp. 775–780, Elsevier, New York.

Kheshgi, H. S., A. K. Jain, R. Kotamarthi, and D. J. Wuebbles (1999), Future atmospheric methane concentrations in the context of the stabilization of greenhouse gas concentrations, *J. Geophys. Res.*, *104*(D16), 19,183–19,190.

Korontzi, S., C. O. Justice, and R. J. Scholes (2003), Influence of timing and spatial extent of savanna fires in southern Africa on atmospheric emissions, *J. Arid Environ.*, *54*, 395–404.

Lacaux, J. P., R. Delmas, and C. Jambert (1996), NO_x emissions from African savanna fires, *J. Geophys. Res.*, *101*(D19), 23,585–23,595.

Lambin, E. F., H. J. Geist, and E. Lepers (2003), Dynamics of land-use and land-cover change in tropical regions, *Annu. Rev. Environ. Resour.*, *28*, 205–241.

Lobert, J., W. C. Keene, J. A. Logan, and R. Yevich (1999), Global chlorine from biomass burning: Reactive Chlorine Emissions Inventory, *J. Geophys. Res.*, *104*(D7), 8373–8389.

Loveland, T. R., and A. S. Belward (1997), The IGBP-DIS global 1 km land cover data set, DISCOVER: First results, *Int. J. Remote Sens.*, *18*, 3291–3295.

Loveland, T. R., Z. Zhu, D. O. Ohlen, J. F. Brown, B. C. Reed, and L. Yang (1999), An analysis of the global cover characterization process, *Photogramm. Eng. Remote Sens.*, *65*, 1021–1032.

Ludwig, J., L. T. Marufu, B. Huber, M. O. Andreae, and G. Helas (2003), Domestic combustion of biomass fuels in developing countries: A major source of atmospheric pollutants, *J. Atmos. Chem.*, *44*, 23–37.

Neftel, A., E. Moor, H. Oeschger, and B. Stauffer (1985), Evidence from polar ice cores for the increase in atmospheric CO_2 in the past two centuries, *Nature*, *315*, 45–47.

Nepstad, D. C., et al. (1999), Large-scale impoverishment of Amazonian forests by logging and fire, *Nature*, *398*, 505–508.

Pereira, J. M. C., B. S. Pereira, P. Barbosa, D. Stroppiana, M. J. P. Vasconcelos, and J. M. Gregoire (1999), Satellite monitoring of fire in the EXPRESSO study area during the 1996 dry season experiment: Active fires, burnt area, and atmospheric emissions, *J. Geophys. Res.*, *104*(D23), 30,701–30,712.

Potter, C., V. Brooks-Genovese, S. Klooster, and A. Torregrosa (2002), Biomass burning emissions of reactive gases estimated from satellite data analysis and ecosystem modeling for the Brazilian Amazon region, *J. Geophys. Res.*, *107*(D20), 8056, doi:10.1029/2000JD000250.

Prather, M., et al. (2001), Atmospheric chemistry and greenhouse gases, in *Climate Change 2001: The Scientific Basis, Contribution of Working Group I to the Third Assessment Report of the Intergovernmental Panel on Climate Change*, edited by J. T. Houghton et al., pp. 239–287, Cambridge Univ. Press, New York.

Radke, L. F., D. A. Hegg, P. V. Hobbs, J. D. Nance, J. H. Lyons, K. K. Laursen, R. E. Weiss, P. J. Riggan, and D. E. Ward (1991), Particulate and trace gas emissions from large biomass fires in North America, in *Global Biomass Burning: Atmospheric, Climatic and Biospheric Implications*, edited by J. S. Levine, pp. 209–224, MIT Press, Cambridge, Mass.

Ramankutty, N., and J. Foley (1998), Characterizing patterns of global land use: An analysis of global croplands data, *Global Biogeochem. Cycles*, *12*(4), 667–685.

Ramankutty, N., and J. A. Foley (1999), Estimating historical changes in global land cover: Croplands from 1700 to 1992, *Global Biogeochem. Cycles*, *13*(4), 997–1027.

Saarnak, C. F., T. T. Nielsen, and C. Mbow (2003), A local scale study of the trace gas emissions from vegetation burning around the village of Dalun, Ghana, with respect to seasonal vegetation changes and burning practices, *Clim. Change*, *56*, 321–338.

Scholes, M. C., and M. O. Andreae (2000), Biogenic and pyrogenic emissions from Africa and their impact on the global atmosphere, *Ambio*, *29*, 23–29.

Scholes, R. J., and B. H. Walker (1993), *An African Savanna: Synthesis of the Nylsvley Study*, Cambridge Univ. Press, New York.

Scholes, R. J., D. E. Ward, and C. O. Justice (1996), Emissions of trace gases and aerosol particles due to vegetation burning in Southern Hemisphere Africa, *J. Geophys. Res.*, *101*(D19), 23,677–23,682.

Schultz, M. G. (2002), On the use of ATSR fire count data to estimate the seasonal and interannual variability in vegetation fire emissions, *Atmos. Chem. Phys.*, *2*, 387–395.

Seiler, W., and P. J. Crutzen (1980), Estimates of gross and net fluxes of carbon between the biosphere and the atmosphere from biomass burning, *Clim. Change*, *2*, 207–247.

Shea, R. W., B. W. Shea, J. B. Kauffman, D. E. Ward, C. I. Haskins, and M. C. Scholes (1996), Fuel biomass and combustion factors associated with fires in savanna ecosystems of South Africa and Zambia, *J. Geophys. Res.*, *101*(D19), 23,551–23,568.

Shirai, T., et al. (2003), Emission estimates of selected volatile organic compounds from tropical savanna burning in northern Australia, *J. Geophys. Res.*, *108*(D3), 8406, doi:10.1029/2001JD000841.

Simon, M., S. Plummer, F. Fierens, J. J. Hoelzemann, and O. Arino (2004), Burnt area detection at global scale using ATSR-2: The GLOBSCAR products and their qualification, *J. Geophys. Res.*, *109*, D14S02, doi:10.1029/2003JD003622.

Sinha, P., P. V. Hobbs, R. J. Yokelson, I. T. Bertschi, D. R. Blake, I. J. Simpson, S. Gao, T. W. Kirchstetter, and T. Novakov (2003), Emissions of trace gases and particles from savanna fires in southern Africa, *J. Geophys. Res.*, *108*(D13), 8487, doi:10.1029/2002JD002325.

Soja, A. J., W. R. Cofer, H. H. Shugart, A. I. Sukhinin, P. W. Stackhouse Jr., D. J. McRae, and S. G. Conard (2004), Estimating fire emissions and disparities in boreal Siberia (1998 through 2002), *J. Geophys. Res.*, *109*, D14S06, doi:10.1029/2004JD004570.

Stocks, B. J., and J. B. Kauffman (1997), Biomass consumption and behavior of wildland fires in boreal, temperate, and tropical ecosystems: Parameters necessary to interpret historic fire regimes and future fire scenarios, in *Sediment Records of Biomass Burning and Global Change*, edited by J. S. Clark, pp. 169–188, Springer, New York.

Susott, R. A., D. E. Ward, R. E. Babbitt, and D. J. Latham (1991), The measurement of trace gas emissions and combustion characteristics for a mass fire, in *Global Biomass Burning: Atmospheric, Climatic, and Biospheric Implications*, edited by J. S. Levine, MIT Press, Cambridge, Mass.

Tansey, K., et al. (2004), Vegetation burning in the year 2000: Global burned area estimates from SPOT VEGETATION data, *J. Geophys. Res.*, *109*, D14S03, doi:10.1029/2003JD003598.

van der Werf, G. R., J. T. Randerson, G. J. Collatz, and L. Giglio (2003), Carbon emissions from fires in tropical and subtropical ecosystems, *Global Change Biol.*, *9*, 547–562.

van der Werf, G. R., J. T. Randerson, G. J. Collatz, L. Giglio, P. S. Kasibhatla, A. Arellano, S. C. Olsen, and E. S. Kasischke (2004), Continental-scale partitioning of fire emissions during the 97/98 El Niño, *Science*, *303*, 73–76.

Ward, D. E., R. A. Susott, J. B. Kauffman, R. E. Babbitt, D. L. Cummings, B. Dias, B. N. Holben, Y. J. Kaufman, R. A. Rasmussen, and A. W. Setzer (1992), Smoke and fire characteristics for Cerrado and deforestation burns in Brazil: BASE-B experiment, *J. Geophys. Res.*, *97*(D13), 14,601–14,619.

Ward, D. E., W. M. Hao, R. A. Susott, R. E. Babbitt, R. W. Shea, J. B. Kauffman, and C. O. Justice (1996), Effects of fuel composition on combustion efficiency and emission factors for African savanna ecosystems, *J. Geophys. Res.*, *101*(D19), 23,569–23,576.

Yevich, R., and J. A. Logan (2003), An assessment of biofuel use and burning of agricultural waste in the developing world, *Global Biogeochem. Cycles*, *17*(4), 1095, doi:10.1029/2002GB001952.

Yokelson, R., R. Susott, D. Ward, J. Reardon, and D. Griffith (1997), Emissions from smoldering combustion of biomass measured by open-path Fourier transform infrared spectroscopy, *J. Geophys. Res.*, *102*(D15), 18,865–18,878.

Yokelson, R. J., J. G. Goode, D. E. Ward, R. A. Susott, R. E. Babbitt, D. D. Wade, I. Bertschi, D. W. T. Griffith, and W. M. Hao (1999), Emissions of formaldehyde, acetic acid, methanol, and other trace gases from biomass fires in North Carolina measured by airborne Fourier transform infrared spectroscopy, *J. Geophys. Res.*, *104*(D23), 30,109–30,125.

Yokelson, R. J., I. T. Bertschi, T. J. Christian, P. V. Hobbs, D. E. Ward, and W. M. Hao (2003), Trace gas measurements in nascent, aged, and cloud-processed smoke from African savanna fires by airborne Fourier transform infrared spectroscopy (AFTIR), *J. Geophys. Res.*, *108*(13), 8478, doi:10.1029/2002JD002322.

Zhu, Z., and E. Waller (2003), Global forest cover mapping for the United Nations Food and Agriculture Organization Forest Resources Assessment 2000 Program, *For. Sci.*, *49*, 369–380.

Zobler, L. (1986), A world soil file for global climate modelling, *NASA Tech. Memo.*, *87802*, 32 pp.

Zobler, L. (1999), Global soil types, 1-degree grid (Zobler): Data set, http://www.daac.ornl.gov, Oak Ridge Natl. Lab. Distrib. Active Archive Cent., Oak Ridge, Tenn.

C. Gillespie, A. K. Jain, Z. Tao, and X. Yang, Department of Atmospheric Science, University of Illinois, 105 South Gregory Street, Urbana, IL 61801, USA. (jain@atmos.iuc.edu)